Mechanism for Visible Light Responses in Anodic Photocurrents at N-Doped TiO_2 Film Electrodes

Ryuhei Nakamura, Tomoaki Tanaka, and Yoshihiro Nakato*

Division of Chemistry, Graduate School of Engineering Science, Osaka University, Toyonaka, Osaka 560-8531, Japan, and Core Research for Evolutional Science and Technology (CREST), Japan Science and Technology Agency (JST)

Received: May 1, 2004; In Final Form: June 4, 2004

Nitrogen doping of anatase TiO_2 powder extended the photocurrent action spectrum for water oxidation from the UV-light region (≤400 nm) to the visible-light region (≤ ∼550 nm), as reported. Investigations of the effect of the addition of reductants such as methanol, SCN^-, Br^-, I^-, and hydroquinone to the electrolyte have for the first time given clear experimental evidence to the mechanism that visible-light responses for N-doped TiO_2 arise from an N-induced midgap level, formed slightly above the top of the (O-2p) valence band. The investigations, in combination with the above mechanism, have also shown that photocatalytic oxidation of organic compounds on N-doped TiO_2 under visible illumination mainly proceed via reactions with surface intermediates of water oxidation or oxygen reduction, not by direct reactions with holes trapped at the N-induced midgap level.

Introduction

Photoinduced oxidation and reduction reactions at the surface of TiO_2 particles or thin films have been attracting much attention in view of their possible application to solar energy conversion (water splitting)[1,2] as well as environmental cleaning (photodecomposition of waste materials and harmful compounds).[3,4] TiO_2 has a high oxidation power under illumination. Also, it is chemically stable, nontoxic, and relatively inexpensive, but it has a serious disadvantage in that it can absorb only UV light.

Recent studies have revealed that the shortcoming of TiO_2 can be overcome by doping it with other elements such as nitrogen,[5,6] sulfur,[7,8] carbon,[9−11] etc. For example, Asahi et al.[5] reported that N-doped TiO_2 showed photocatalytic activity for the decomposition of acetone and methylene blue in wavelengths up to 550 nm. Khan et al.[9] also reported that carbon doping of TiO_2 extended the photoactive region for water oxidation from 400 to 535 nm, thus leading to a large increase in the water-splitting efficiency under white-light illumination.

The method of doping is thus indeed effective, but we have to note that some problems may arise from this method. It is widely recognized[12] that doping of metal oxides with other elements produces electronic midgap states associated with dopants. The trapping of photogenerated holes at such midgap states will cause a decrease in their oxidation power. In addition, the doping may induce instability of the TiO_2, owing to the introduction of lattice distortion and bond weakening. It is thus important to investigate the mechanism of photooxidation reactions and stability for doped TiO_2, compared with those[3,4,13−15] for nondoped TiO_2. To date, a number of studies have been conducted[16−23] on the origin of the visible-light responses for doped TiO_2, but no clear experimental evidence has been given; thus, a definite mechanism still seems to remain in dispute. In the present paper, we report a definite mechanism for the visible-light responses in water photooxidation (oxygen photoevolution) on N-doped TiO_2, as revealed by photocurrent measurements with film electrodes.

Experimental Section

N-doped TiO_2 powder was prepared by dry[5] and wet[6] methods. In the dry method, anatase TiO_2 powder (ST01, Ishihara Sangyo Co.) was heated at 550 °C in an alumina tube reactor under dry NH_3 gas flow for 3 h. This sample will hereafter be called sample A. In the wet method, 100 mL of an aqueous solution of 28% ammonia was added dropwise to 25 mL of 95.0% titanium tetraisopropoxide (TTIP) at 0 °C with stirring, and the resulting precipitate was washed well with pure water. After evaporation of water, the white precipitate was gradually heated in air to raise the temperature slowly at a rate of 1 °C/min up to 400 °C, followed by maintaining at 400 °C for 6 h.[6] The slow temperature raise was important for getting high photoactivity. This sample will be called sample B.

Film electrodes of N-doped TiO_2 for photocurrent measurements were prepared as follows: N-doped TiO_2 powder (0.25 g) was ground in a mortar for 1 h with 0.5 mL of water and 0.1 mL of acetylacetone, and it was then transferred to 5 mL of 1.5% HNO_3 under stirring, followed by addition of Triton X-100 at a ratio of 0.5 g per 20 mL solution. A resultant colloidal TiO_2 solution was applied on transparent conductive oxide (F-doped SnO_2) films on glass plates (Nippon Sheet Glass Co. Ltd., resistance of ∼20 Ω/square) using a spin coater at 2000 rpm, and these were heated at 150 °C with an electric furnace. This procedure was repeated six times, and the TiO_2 films thus obtained were finally heated at 400 °C for 3 h in air. A copper wire was attached on an edge of the F−SnO_2 film with silver paste, and the whole part, except a 1.0 × 1.0 cm^2 TiO_2 film area, was covered with epoxy resin for insulating.

Photocurrents for nondoped and N-doped TiO_2 film electrodes were measured as a function of wavelength (λ), using a 350 W xenon lamp (Ushio) as the light source and a monochromator (Bunkoh-Keiki Co., M10-T) with a bandwidth of 10 nm. The incident photon to current efficiency (IPCE) was calculated from the photocurrent by an equation

10.1021/jp048112q CCC: $27.50
Published on Web 06/26/2004

$$\text{IPCE}\ (\lambda) = 1240 \times j(\lambda)/\lambda I_0(\lambda) \times 100 \qquad (1)$$

where λ is the wavelength of light in units of nm, $j(\lambda)$ is the photocurrent density in mA cm^{-2} under illumination at λ, and $I_0(\lambda)$ is the incident-light intensity in mW cm^{-2} at λ. A Pt plate was used as the counter electrode, and an Ag/AgCl/sat. KCl electrode was used as the reference electrode.

Results and Discussion

X-ray diffraction (XRD) analysis demonstrated that both samples A and B had an anatase form. Scanning electron microscopy (SEM) inspection showed that the film of sample A was ~3 μm thick and composed of TiO_2 particles of 0.2−1.0 μm in diameter, while that of sample B was ~5 μm thick and composed of particles of 0.5−1.5 μm in diameter. Both samples A and B exhibited a pale yellow color. In fact, the UV−visible absorption spectra for both samples showed a shoulder band at around 440 nm, indicating that nitrogen is really doped. However, X-ray photoelectron spectroscopy (XPS) analysis showed no clear N-1s peak at 396 eV, assignable to the nitrogen of Ti−N bonds,[19,21] probably owing to a too small amount of nitrogen atoms in the N-doped TiO_2 film, though an N-1s peak at 400 eV, probably assignable to adsorbed nitrogen compounds such as NO_x[24] or NH_x[22], was observed.

Figure 1 shows the IPCE vs λ plot for an N-doped TiO_2 (sample A) film electrode in 0.1 M $HClO_4$ compared with that for a nondoped TiO_2 (ST01) film. The nitrogen doping caused an extension of the photoresponse up to ~550 nm, as reported.[5,6] Since the electrolyte contains only indifferent (stable) ions, the observed photocurrents for both electrodes can be attributed to photooxidation of water (photoevolution of oxygen), though it was difficult to detect evolved oxygen experimentally, owing to a low current density.

Figure 2 shows the effect of the addition of 6 M methanol to the electrolyte (0.1 M $HClO_4$). The IPCE for N-doped TiO_2 (sample A) under UV illumination exhibited a large increase by a factor of 6−7 by the addition of methanol (Figure 2a), whereas that under visible-light illumination exhibited only a little increase by a factor of 1.1−1.4 (Figure 2b). Similarly, Figure 3 shows the effect of the addition of other reductants such as 0.5 mM I^-, hydroquinone (H_2Q), SCN^-, and Br^-. The IPCE under UV illumination was increased by the addition of all the reductants (Figure 3a), whereas that under visible-light illumination was increased only by the addition of I^- and H_2Q (Figure 3b).

We did similar experiments on sample B and obtained quite the same results as those for sample A. This indicates that the difference in the enhancement of the IPCE by the addition of reductants between the visible- and UV-light irradiation is not due to a particular method of sample preparation but rather arises from the nitrogen doping itself.

As to the origin of visible-light responses for N-doped TiO_2, different groups have proposed different mechanisms to date and no definite conclusion has been obtained yet, as mentioned in the Introduction section. For example, Asahi et al.[5] reported, on the basis of calculations of band structures, that visible-light responses for $TiO_{2-x}N_x$ ($x = 0.25$ and 0.12) arose from band narrowing by mixing of N-2p and O-2p orbitals. Ihara et al.[18] reported that N-doped TiO_2 powder contained not only nitrogen but also oxygen vacancies and electronic levels due to the oxygen vacancies, lying slightly below the conduction band edge, were responsible for visible-light responses. Irie et al. reported[19] that $TiO_{2-x}N_x$ with $0.005 \le x < 0.02$ showed low activity for the photooxidation of 2-propanol under visible-light irradiation, compared with UV irradiation, similar to the present work, and explained the result as being due to the formation of an N-induced narrow band slightly above the top of the valence band. The conclusion of Irie et al. was, however, not decisive because their used method of product analysis included serious problems, as explained later. On the other hand, Sakatani et al. reported,[20] using electron spin resonance (ESR) measurements, that the visible responses arose from paramagnetic nitrogen species (such as NO, NO_2, etc.) that were existing initially in the dark and produced by UV and visible irradiation, though without showing any electronic band structure. However, Diwald et al. reported very recently,[22] using XPS analysis, that doped nitrogen was existing in the form of NH_x in single crystal TiO_2 (rutile). In addition, Ihara et al. reported,[18] using diffuse reflection IR spectroscopy, that NO_2, NO, and NH_3 were produced at the surface of N-doped TiO_2 in the course of its preparation.

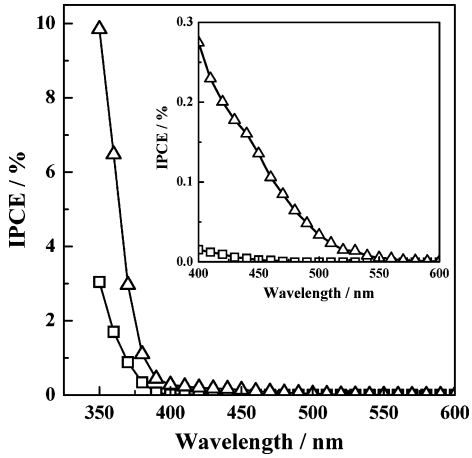

Figure 1. IPCE vs λ for (△) N-doped TiO_2 (sample A) and (□) nondoped TiO_2 (ST01) in 0.1 M $HClO_4$ at 0.5 V vs Ag/AgCl. The inset shows an expanded plot of IPCE vs λ in the visible-light region.

In the present work, we have measured anodic photocurrents that arise only from photooxidation reactions, in contrast to the case of photoreaction products, and succeeded in obtaining a definite conclusion on the mechanism. First, let us consider why the IPCE is enhanced by the addition of a reductant to the electrolyte. Oxygen photoevolution reaction on TiO_2 in the absence of reductants produces a number of surface reaction intermediates,[25,26] leading to efficient carrier recombination especially in powdered systems without any band bending. On the other hand, photooxidation reactions of reductants such as methanol, I^-, H_2Q, SCN^-, and Br^- by photogenerated holes in general proceed effectively with much less surface intermediates, which leads to much less carrier recombination and hence high IPCEs. In addition, for methanol, a current doubling mechanism[27] may contribute to the increase in the IPCE.[28]

We mentioned earlier that all reductants added [such as methanol, I^-, hydroquinone (H_2Q), SCN^-, and Br^-] increased the IPCE under UV illumination, whereas only I^- and H_2Q increased the IPCE under visible-light illumination (Figures 2 and 3). This result implies, on the basis of the above argument, that all the reductants are oxidized under UV illumination, whereas only I^- and H_2Q are oxidized under visible-light illumination. The reduced oxidation power under visible illumination relative to UV illumination can never be explained by the reported concepts of band narrowing[5] or formation of the oxygen-vacancy levels slightly below the conduction band edge.[18] The reduced oxidation power can only be explained by the mechanism that the doped nitrogen species (such as NH_x[22])

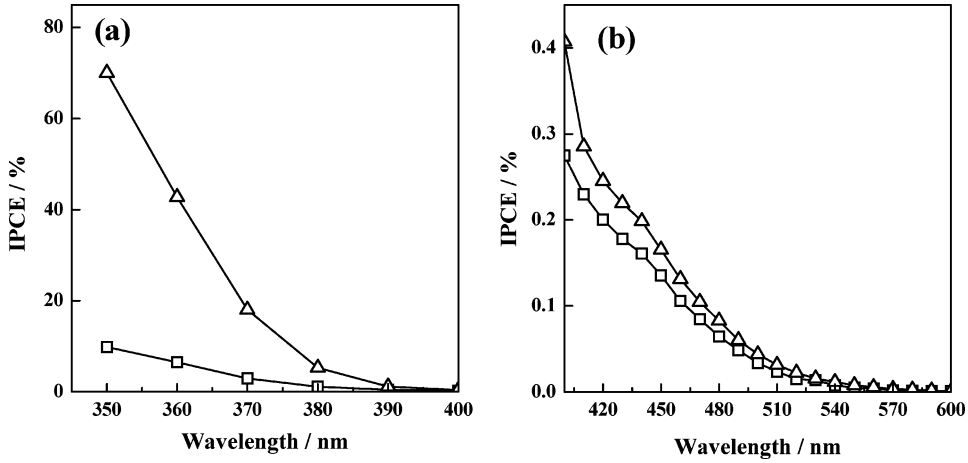

Figure 2. IPCE vs λ for N-doped TiO_2 (sample A) in 0.1 M $HClO_4$ (△) with and (□) without 6 M methanol in the (a) UV- and (b) visible-light regions. The electrode potential was 0.5 V vs Ag/AgCl.

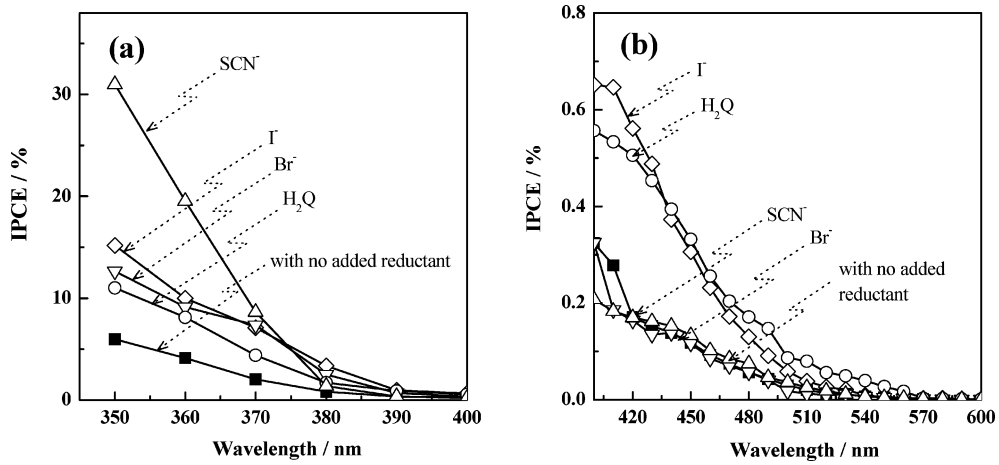

Figure 3. Effect of the addition of 0.5 mM I^-, H_2Q, SCN^-, and Br^- as a reductant on the plot of IPCE vs λ in the (a) UV- and (b) visible-light regions for N-doped TiO_2 (sample A) in 0.1 M $HClO_4$. The electrode potential was 0.5 V vs Ag/AgCl.

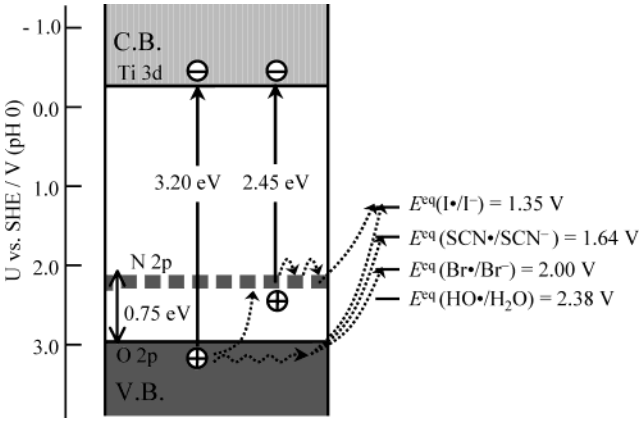

Figure 4. Schematic illustration of the expected energy bands for N-doped TiO_2 (anatase) together with some photoinduced electronic processes. C.B., conduction band; V.B., valence band; minus sign with a circle, electron; plus sign with a circle, hole; E^{eq}, reported equilibrium redox potentials[29] for one-electron-transfer redox couples indicated in parentheses in the figure.

give rise to a (occupied) midgap (N-2p) level slightly above the top of the (O-2p) valence band and visible-light illumination produces "holes" in the midgap level, whereas UV illumination produces holes in the (O-2p) valence band, as shown in Figure 4. The differences in the IPCE enhancement between UV and visible illumination can be attributed to differences in the reactivity of these holes.

It is worthwhile to note here that the photocurrent measurement is crucially important for getting definite conclusions on the reaction mechanism. Product analysis, often used in the literature for photocatalytic reactions in powdered systems, cannot distinguish whether a reaction product comes from a photooxidation process or a photoreduction process. Moreover, product analysis cannot determine whether a certain product of the oxidation of an organic compound comes from a direct reaction with photogenerated holes or via reactions with surface intermediates (such as the Ti−O• radical) of the water photooxidation reaction. It is thus quite difficult to get definite conclusions on the reaction mechanism from product analysis. On the other hand, photocurrent measurement can in general distinguish the above two oxidation processes because the photocurrent largely increases if a direct reaction with photogenerated holes occurs, whereas it hardly increases if an indirect reaction via the intermediates of water photooxidation occurs (Figures 2 and 3). It has been reported from product analysis that a variety of organic compounds such as methylene blue,[5] 2-propanol,[19] and acetone[5,20] are oxidized into CO_2 on N-doped TiO_2 by visible-light illumination, whereas the photocurrent measurements in the present work show that even readily oxidized methanol is hardly oxidized by the visible-light illumination (Figure 2). Such a discrepancy strongly suggests that most of the photocatalytic oxidation reactions of organic compounds in powdered N-doped TiO_2 systems proceed via surface intermediates of oxygen reduction or water oxidation,

not via direct reactions with holes trapped at the N-induced midgap level. The discrepancy thus indicates clearly the limitation of the method of product analysis.

Finally, let us consider why holes trapped in the N-induced midgap level can only oxidize I^- and H_2Q, though holes in the (O-2p) valence band can oxidize all the reductants (Figures 3). In relation to this fact, we also have to note that the holes at the N-induced level, which cannot oxidize Br^- and SCN^- (Figure 3), can oxidize water (Figure 1). The former result may be explained by comparing the reported one-electron-transfer equilibrium redox potentials[29] for reductants with the energies for the midgap N level and the valence band for N-doped TiO_2, which could be estimated from the reported flat band potential[16] and the conduction band edge[17] (Figure 4). We can expect that the more negative the redox potential of a reductant, the more easily oxidized the reductant is. In fact, the I•/I^- redox level is considerably above the N-induced midgap level, suggesting that I^- can be easily oxidized, in agreement with the experiment. We have no reported datum for the one-electron-transfer redox level for H_2Q. Little reactivity for SCN^- and Br^-, whose redox level lies above the midgap N level (Figure 4), can probably be attributed to the presence of large reorganization energies[30] in the electron-transfer reaction for such small ions in aqueous media.

Now, why is water oxidized by the holes trapped at the N-induced midgap level, in spite of the fact that the redox potential for water oxidation (HO•/H_2O) is far below this level (Figure 4)? This keen contradiction can be solved if we take into account that the water oxidation is not caused by an electron-transfer type reaction. Very recently, we reported,[31,32] by using in-situ Fourier transform infrared (FTIR) and photoluminescence (PL) measurements, that water photooxidation on *n*-TiO_2 (rutile) is not initiated by the oxidation of the surface OH group (Ti−OH_s) with photogenerated holes (h^+)

$$\mathrm{Ti{-}OH_s} + \mathrm{h^+} \rightarrow [\mathrm{Ti \bullet OH}]_s^+ \qquad (2)$$

but initiated by a nucleophilic attack of an H_2O molecule (Lewis base) to a surface hole (Lewis acid), accompanied by bond breaking.

$$[\mathrm{Ti{-}O{-}Ti}]_s + \mathrm{h^+} + \mathrm{H_2O} \rightarrow [\mathrm{Ti{-}O\bullet\ HO{-}Ti}]_s + \mathrm{H^+} \qquad (3)$$

The easiness of occurrence of reaction 3 will not have any direct relation with the redox potential such as E_{eq}(HO•/H_2O) in Figure 4 but will have a strong relation with the basicity of H_2O or the energy of an intermediate radical $[Ti{-}O\bullet\ HO{-}Ti]_s$ that is roughly giving the activation energy for the reaction. In other words, the above-mentioned contradiction can be regarded as giving strong support to the validity of our previously reported[31,32] mechanism for the water photooxidation on TiO_2.

The above arguments indicate that the oxidation power of surface holes strongly depends on the reaction mechanism, and we cannot discuss it without knowledge on the mechanism. In relation to this statement, it is interesting to note that the large IPCE enhancements by reductants under UV illumination relative to visible illumination (Figures 2 and 3) show that most of the holes generated in the (O-2p) valence band for N-doped TiO_2 can escape from trapping at the N-induced midgap level and reach the surface and directly react with the solution (Figure 4). The result is quite strange in view of a conventional concept that valence band holes are in general effectively trapped by an impurity midgap state. Detailed investigations of the mechanism will give new insights into an understanding of the valence band holes and impurity-level holes and their mutual interactions.

In conclusion, the present work has given definite evidence for the mechanism that visible-light responses for N-doped TiO_2 arise from formation of an N-induced (occupied) midgap level slightly above the valence band edge. Investigations of the effect of the addition of various reductants to the electrolyte have revealed that the oxidation power of surface holes strongly depends on the reaction mechanism and we cannot discuss it without knowledge on the mechanism. The investigations have also clarified the limitation of the method of product analysis that has often been used in the literature to elucidate reaction mechanisms.

References and Notes

(1) Fujishima, A.; Honda, K. *Nature* **1972**, *238*, 37.
(2) Sato, S.; White, M. *Chem. Phys. Lett*. **1980**, *72*, 83.
(3) Hoffmann, M. R.; Martin, S. T.; Choi, W.; Bahnemann, D. W. *Chem. Rev*. **1995**, *95*, 69.
(4) Ollis, D. F., Al-Ekabi, H., Eds. *Photocatalytic Purification and Treatment of Water and Air*; Elsevier: Amsterdam, The Netherlands, 1993.
(5) Asahi, R.; Morikawa, T.; Ohwaki, T.; Aoki, K.; Taga, Y. *Science* **2001**, *293*, 269.
(6) Sato, S. *Chem. Phys. Lett*. **1986**, *123*, 126.
(7) Umebayashi, T.; Yamaki, T.; Itoh, H.; Asai, K. *Appl. Phys. Lett*. **2002**, *81*, 454.
(8) Ohno, T.; Mitsui, T.; Matsumura, M. *Chem. Lett*. **2003**, *32*, 364.
(9) Khan, S. U. M.; Al-Shahry, M.; Ingler, W. B., Jr. *Science* **2002**, *297*, 2243.
(10) Sakthivel, S.; Kisch, H. *Angew. Chem., Int. Ed*. **2003**, *42*, 4908.
(11) Irie, H.; Watanabe, Y.; Hashimoto, K. *Chem. Lett*. **2003**, *32*, 772.
(12) Diebold, U. *Surf. Sci. Rep*. **2003**, *48*, 53.
(13) Nakamura, R.; Imanishi, A.; Murakoshi, K.; Nakato, Y. *J. Am. Chem. Soc*. **2003**, *125*, 7443.
(14) Tsujiko, A.; Kisumi, T.; Magari, Y.; Murakoshi, K.; Nakato, Y. *J. Phys. Chem. B* **2000**, *104*, 4873.
(15) Nakato, Y.; Akanuma, H.; Magari, Y.; Yae, S.; Shimizu, J.-I.; Mori, H. *J. Phys. Chem. B* **1997**, *101*, 4934.
(16) Sakthivel, S.; Kisch, H. *ChemPhysChem* **2003**, *4*, 487.
(17) Lindgren, T.; Mwabora, J. M.; Avendanño, E.; Jonsson, J.; Hoel, A.; Granqvist, C.-G.; Lindquist, S.-E. *J. Phys. Chem. B* **2003**, *107*, 5709.
(18) Ihara, T.; Miyoshi, M.; Iriyama, Y.; Matsumoto, O.; Sugihara, S. *Appl. Catal., B* **2003**, *42*, 403.
(19) Irie, H.; Watanabe, Y.; Hashimoto, K. *J. Phys. Chem. B* **2003**, *107*, 5483.
(20) Sakatani, Y.; Nunoshige, J.; Ando, H.; Okusako, K.; Koike, H.; Takata, T.; Kondo, J. N.; Hara, M.; Domen, K. *Chem. Lett*. **2003**, *32*, 1156.
(21) Diwald, O.; Thompson, T. L.; Goralski, E. G.; Walck, S. D.; Yates, J. T., Jr. *J. Phys. Chem. B* **2004**, *108*, 52.
(22) Diwald, O.; Thompson, T. L.; Zubkov, T.; Goralski, E. G.; Walck, S. D.; Yates, J. T., Jr. *J. Phys. Chem. B* **2004**, *108*, 6004.
(23) Torres, R. G.; Lindgren, T.; Lu, J.; Granqvist, C.-G.; Lindquist, S.-E. *J. Phys. Chem. B* **2004**, *108*, 5995.
(24) Rodriguez, J. A.; Jirsak, T.; Dvorak, J.; Sambasivan, S.; Fischer, D. *J. Phys. Chem. B* **2000**, *104*, 319.
(25) Wilson, R. H. *J. Electrochem. Soc*. **1980**, *127*, 228.
(26) Ulmann, M.; Tacconi, N. R.; Augustynski, J. *J. Phys. Chem*. **1986**, *90*, 6523.
(27) Morrison, S. R.; Freund, T. *J. Chem. Phys*. **1967**, *47*, 1543.
(28) Shiga, A.; Tsujiko, A.; Yae, S.; Nakato, Y. *Bull. Chem. Soc. Jpn*. **1998**, *71*, 2119.
(29) Wardman, P. *J. Phys. Chem. Ref. Data* **1989**, *18*, 1637.
(30) Burg, V. K.; Delahay, P. *Chem. Phys. Lett*. **1981**, *78*, 287.
(31) Kisumi, T.; Tsujiko, A.; Murakoshi, K.; Nakato, Y. *J. Electroanal. Chem*. **2003**, *545*, 99.
(32) Nakamura, R.; Nakato, Y. *J. Am. Chem. Soc*. **2004**, *126*, 1290.